

Domain Adaptive Semantic Segmentation without Source Data: Align, Teach and Propagate

Yuxi Wang^{1,2} Jian Liang² Jun Xiao¹ Yuran Yang⁴ Shuqi Mei⁴ Zhaoxiang Zhang^{1,2,3,*}

¹ University of Chinese Academy of Sciences

² Center for Research on Intelligent Perception and Computing, CASIA

³ Center for Excellence in Brain Science and Intelligence Technology, CAS, ⁴ Tencent Map, T Lab

{wangyuxi2016, zhaoxiang.zhang}@ia.ac.cn, xiaojun@ucas.ac.cn

liangjian92@gmail.com, {yuranyang, shawnmei}@tencent.com

Abstract

Benefiting from considerable pixel-level annotations collected from a specific situation (source), the trained semantic segmentation model performs quite well but fails in a new situation (target) due to the large domain shift. To mitigate the domain gap, previous cross-domain semantic segmentation methods always assume the co-existence of source data and target data during domain alignment. However, the accessing to source data in the real scenario may raise privacy concerns and violate intellectual property. To tackle this problem, we focus on an interesting and challenging cross-domain semantic segmentation task where only the trained source model is provided to the target domain. Specifically, we propose a unified framework called **ATP**, which consists of three schemes, i.e., feature **Alignment**, bidirectional **Teaching**, and information **Propagation**. First, we devise a curriculum-style entropy minimization objective to implicitly align the target features with unseen source features via the provided source model. Second, besides positive pseudo labels in vanilla self-training, we are among the first ones to introduce negative pseudo labels to this field and develop a bidirectional self-training strategy to enhance the representation learning in the target domain. Finally, the information propagation scheme is employed to further reduce the intra-domain discrepancy within the target domain via pseudo semi-supervised learning. Extensive results on synthesis-to-real and cross-city driving datasets validate **ATP** yields state-of-the-art performance, even on par with methods that need access to source data.

1. Introduction

Semantic segmentation is a fundamental task in the computer vision field that aims to estimate the pixel-level predic-

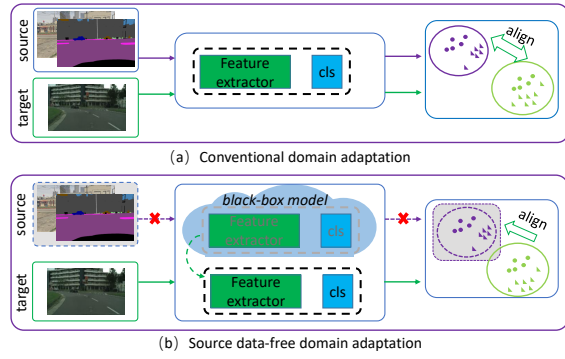


Figure 1. Comparison between the conventional and source data-free domain adaptation for semantic segmentation. The proposed source data-free domain adaptation method only relies on the trained source model, while the conventional methods require all the labeled source data and the target data. Moreover, the black-box model that only the source model’s predictions are available can also perform well.

tions for a given image. Despite the rapid progress on deep learning-based methods, attaining high performance usually demands vast amounts of training data with pixel-level annotations. However, collecting large-scale datasets tends to be prohibitively expensive and time-consuming. Alternatively, previous cross-domain learning approaches [26, 27, 40, 43, 49] attempt to train a satisfactory segmentation model for unlabeled real-world data (called target domain) by exploiting labeled photo-realistic synthetic images (called source domain). However, due to the domain discrepancy, a well-performing model trained on the source domain degrades drastically when applied to the target domain. To remedy this issue, various domain alignment strategies are proposed in [4, 12, 13, 21, 40, 44].

The essential idea for domain adaptive semantic segmentation is to effectively transfer knowledge from a distinct source domain to a target domain. Previous methods

*Corresponding author

achieve this goal by bridging the domain gap in the image level [5, 8, 12, 16, 49], feature level [2, 4, 13], and output level [27, 40, 41, 43]. Although these approaches have made remarkable progress, they usually require access to the labeled source data during the alignment process. However, in some crucial scenarios, the source data is inaccessible due to data protection laws. Thus, this paper addresses a challenging and interesting source data-free domain adaptation issue, where only the trained source model instead of the source data is provided to the target domain for adaptation.

Training a source data-free adaptation model is more challenging compared to conventional unsupervised domain adaptation approaches. As Figure 1 shows, due to the absence of source data, previous domain alignment methods are not feasible anymore. Moreover, the generated pseudo labels are not reliable because of the performance degradation. Although recent works attempt to address this problem by model adaptation [14, 35] or estimating the source data [25], they highly rely on the prior knowledge of the source model and partially ignore the target-specific information, leading to sub-optimal solutions.

In this paper, we propose a new framework called **ATP**, which focuses on exploiting the target knowledge for adaptation. Specifically, three pivotal factors are introduced to guide the procedure, namely implicit feature alignment, bidirectional self-training, and information propagation. The implicit feature alignment scheme aims to ensure the target features are aligned with the source features through hypothesis transfer [22]. Considering hard samples perform poorly due to domain discrepancy, explicitly emphasizing these samples at the early training stage may lead to the convergence issue. To address this, we incorporate the idea of Curriculum Learning (CL) [54, 57] into domain adaptation. We develop a curriculum-style entropy loss to automatically emphasize easy samples first and hard samples later. During the bidirectional self-training process, we are among the first ones to introduce negative pseudo-labeling to the domain adaptation field. Specifically, the negative pseudo labels refer to the predictions with low confidence scores, providing solid supervised information to indicate the absent classes for the corresponding pixels. We further consider vanilla positive pseudo labels with high confidence scores and develop a bidirectional self-training strategy to enhance the target representation learning. Finally, the information propagation scheme aims to reduce intra-domain discrepancy within the target domain. Particularly, we conduct a proxy semi-supervised learning task for target data and integrate dominant techniques to boost the performance. This propagation acts as a generic simple and effective post-processing module for domain adaptation.

The main contributions of this paper can be summarized as follows. 1) We propose a novel source data-free domain adaptation method for semantic segmentation that only re-

quires the source model and unlabeled target data. The proposed method can also perform well on the black-source model, where only the source model’s predictions are available. 2) We develop a novel curriculum-style entropy objective for implicitly aligning the features of source and target domains. 3) We propose a new bidirectional self-training strategy that considers both the positive pseudo labeling and negative pseudo labeling. 4) The proposed method yields state-of-the-art cross-domain results with the Cityscapes [9] segmentation mIoU by 52.6 and 57.9 when adapting from GTA5 [33] and SYNTHIA [34].

2. Related Work

Domain Adaptive Semantic Segmentation. Existing domain adaptation methods for semantic segmentation can be roughly categorized into two groups: adversarial learning based methods and self-supervised learning based methods. For adversarial learning, numerous works focus on reducing the distribution misalignment in the image level [5, 8, 12, 15, 16, 37, 45, 49], feature level [2, 4, 13], and output level [27, 40, 41, 43]. For the self-supervised learning method, the essential idea is to generate reliable pseudo labels. Typical approaches usually consist of two steps: 1) generate pseudo labels based on the source model [28, 56, 57] or the learned domain-invariant model [20, 38, 55], 2) refine the target model supervised by the generated pseudo labels [44, 52]. Moreover, [36] and [39] provide a new unaligned score to measure the efficiency of a learned model on a new target domain. Although these methods have achieved promising results, they usually depend heavily on the labeled source data during adaptation. In this paper, we address a challenging source data-free domain adaptation without any raw source data due to the data privacy policy.

Source Data-free Domain Adaptation. To tackle source data-free domain adaptation problem, a few recent methods [7, 19, 22, 46, 48] provide kinds of model adaptation solutions for classification problems. [18] proposes a universal source data-free domain adaptation when the knowledge of the label space in the target domain is not available. As for semantic segmentation tasks, model adaptation is also a feasible method to tackle the source data absent setting. Specifically, [25] leverages a generative model to synthesize fake samples to estimate the source distribution and preserve source domain knowledge via knowledge transfer during model adaptation. [35] proposes an uncertainty-reducing method to enhance feature representation. [17] and [50] achieve promising performance via generating a generalized source model trained by data augmentation strategies. In contrast, we propose a simple and effective framework for semantic segmentation tasks, exploiting the target-specific knowledge to intensify the target feature learning.

Semi-supervised Learning. The key for semi-supervised learning is to learn a consistent representation

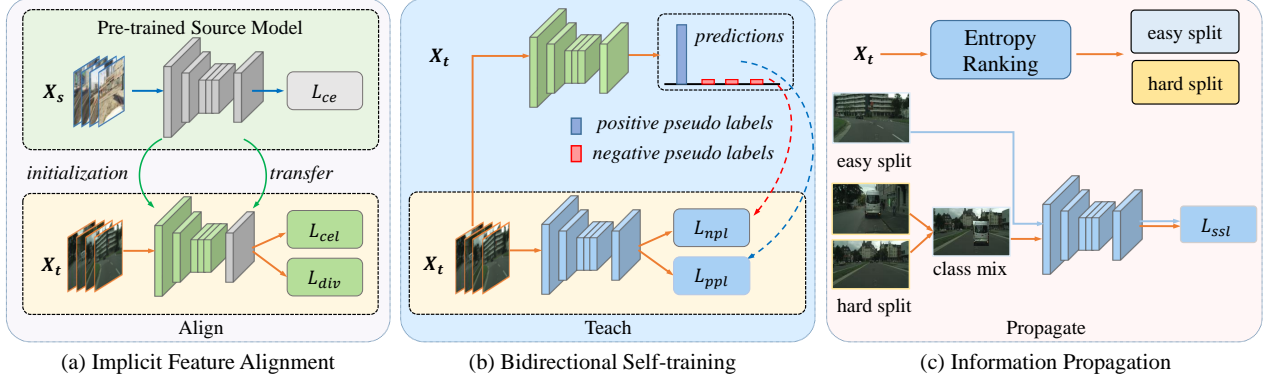


Figure 2. Illustration of the proposed align, teach, and propagate (**ATP**) framework for domain adaptive semantic segmentation without source data. (a) is the implicit feature alignment. We freeze the classifier and train the feature extractor to achieve implicit feature alignment by minimizing \mathcal{L}_{cel} and \mathcal{L}_{div} . (b) illustrates the process of bidirectional self-training. Positive and negative pseudo labels are obtained from a fixed model initialized from stage (a). (c) illustrates the process of information propagation. The target data is divided into easy and hard splits according to the entropy ranking, and then we reduce intra-domain discrepancy in a semi-supervised manner by minimizing loss \mathcal{L}_{ssl} .

between the labeled and unlabeled data. To achieve this goal, consistency regularization methods have been heavily studied in recent years. [29] first introduces perturbations into the input that changes output predictions mostly. Then the augmentation is adopted as solid perturbations. [42] uses the Mixup as the consistency regularization. [47] uses auto-augmentation to generate augmented inputs, and [1] extends the idea by dividing the augmentation set into strong and weak operations. In this work, we refer to the semi-supervised learning strategy to domain adaptation, aiming to reduce the intra-domain discrepancy within the target domain.

3. Method

We aim to address source-data absent domain adaptive semantic segmentation with only a pre-trained source model in this paper. Specifically, we are given n_s labeled images $\{x_s^i, y_s^i\}_{i=1}^{n_s}$ from the source domain \mathcal{D}_s and n_t unlabeled images $\{x_t^i\}_{i=1}^{n_t}$ from the target domain \mathcal{D}_t , where $x_s^i \in \mathcal{X}_s$, $y_s^i \in \mathcal{Y}_s$, and $x_t^i \in \mathcal{X}_t$. Our goal is to learn a segmentation mapping $\mathcal{M}_t : \mathcal{X}_t \rightarrow \mathcal{Y}_t$ transferring from the source mapping $\mathcal{M}_s : \mathcal{X}_s \rightarrow \mathcal{Y}_s$, which predicts a pixel-wise label $y_t^i \in \mathcal{Y}_t$ for a given image x_t^i . In this work, we only access target images $\{x_t^i\}_{i=1}^{n_t}$ and the source mapping \mathcal{M}_s during training.

The semantic segmentation model \mathcal{M}_s on the source domain is obtained in a supervised manner by minimizing the following cross-entropy loss,

$$\mathcal{L}_{ce} = -\frac{1}{n_s} \sum_{i=1}^{n_s} \sum_{j=1}^{H \times W} \sum_{c=1}^C y_s^{(i,j,c)} \log p_s^{(i,j,c)}, \quad (1)$$

where n_s is the number of source images, H and W denote the image size, and C is the number of categories. $p_s^{(i,j,c)}$

denotes the predicted category probability by \mathcal{M}_s and the $y_s^{(i,j,c)}$ is the corresponding one-hot ground-truth label. Generally, the segmentation model \mathcal{M}_s consists of a feature extractor f_s and a classifier g_s , i.e., $\mathcal{M}_s = f_s \circ g_s$.

To transfer the trained \mathcal{M}_s to the target domain, our proposed **ATP** framework mainly includes three stages, shown in Figure 2. The implicit feature alignment implicitly enforces the target feature to fit the source model via the proposed curriculum-style entropy minimization and weighted diversity loss, referring to Sec. 3.1. In this stage, the target model is initialized by \mathcal{M}_s and the classifier is frozen during training. During self-training process, we enhance target feature representation learning by the proposed bidirectional self-training technique described in Sec. 3.2. Finally, we achieve information propagation in a semi-supervised manner, which reduces the intra-domain discrepancy and boosts the adaptation performance with a significant improvement.

3.1. Implicit Feature Alignment

To eliminate the domain gap, entropy minimization strategy is adopted for training. Although previous methods [31, 43] have demonstrated the effectiveness of entropy minimization, they are not appropriate for the source data-free setting because they treat equal importance for different samples. However, hard-to-transfer samples with uncertain predictions (high entropy values) may deteriorate the target feature learning procedure. To address this issue, we attempt to explore more reliable supervision from the easy-to-transfer examples with certain predictions (lower entropy values). Inspired by the curriculum learning algorithm [54, 57], we focus the target data training on automatically emphasizing the easy samples first and hard samples later. Specifically, we exploit a curriculum-style entropy loss that expects to rapidly focus the model on certain predictions and down-weight the contribution of uncertain predictions. Formally,

the curriculum-style entropy loss is formulated as follows:

$$\mathcal{L}_{cel} = \alpha * (1 - h(x_t))^\gamma * h(x_t), \quad (2)$$

where α balances the importance of certainty/uncertainty predictions and γ controls the weight of certainty samples. $h(x_t) = -\sum_{c=1}^C p_{x_t}^{(h,w,c)} \log p_{x_t}^{(h,w,c)}$ denotes the entropy map and $p_{x_t}^{(h,w,c)}$ is the predicted probability of the target image x_t , *i.e.*, $p_{x_t}^{(h,w,c)} = f_t \circ g_t(x_t)$. f_t and g_t denote the feature extractor and classifier for the target data. Weights of hard-to-transfer samples with higher $h(x_t)$ are reduced and easy samples are emphasized relatively. During training, we pursue hypothesis transfer [22] by fixing classifier module to implicitly align the target features with the source features, *i.e.*, $g_t = g_s$. As we utilize the same classifier module for different domain-specific features, the optimal target features are enforced to fit the source feature distribution as they should have a similar one-hot encoding output. Experiments in Sec. 4 reveal this strategy is important.

From the above loss, the trained model concentrates more on easy-to-transfer classes with a slight domain gap or a large pixel proportion, which may lead to a trivial solution with under-fitting on hard-to-transfer classes. To tackle this issue, we develop a diversity-promoting loss to ensure the global diversity of the target outputs. Exactly, we expect to see the prediction of the target output containing all categories. The proposed confidence-weighted diversity objective is below,

$$\mathcal{L}_{div} = \sum_{c=1}^C \hat{p}_{x_t}^{(h,w,c)} \log \hat{p}_{x_t}^{(h,w,c)}, \quad (3)$$

where $\hat{p}_{x_t}^{(h,w,c)}$ is the weighted mean output embedding of the target image x_t . The weight is calculated based on the entropy $h(x_t)$ and $\hat{p}_{x_t}^{(h,w,c)} = \sum_{(h,w)} \exp(-\lambda * h(x_t)) * p_{x_t}^{(h,w,c)}$. λ is a hyper-parameter and we empirically set $\lambda = 3$ in all experiments. By diversifying the output of target prediction, this technique can circumvent the problem of wrongly predicting confusing target instances as relatively easy classes to learn.

3.2. Bidirectional Self-training

Previous self-supervised learning methods focus on strengthening the reliability of pseudo labels by developing various denoising strategies [44, 52], but they ignore most of the pixels with lower prediction confidence scores. In that case, the model tends to be over-fitting because the selected over-confident samples lack references using negative pseudo labels. To remedy this, we restrict our attention to the predictions with lower confidence values, termed negative pseudo labels. Although low-confidence predictions cannot be assigned as the correct labels, they will definitely indicate specific absent classes. As Figure 3 shows, it is hard to clearly indicate which category it belongs to for the

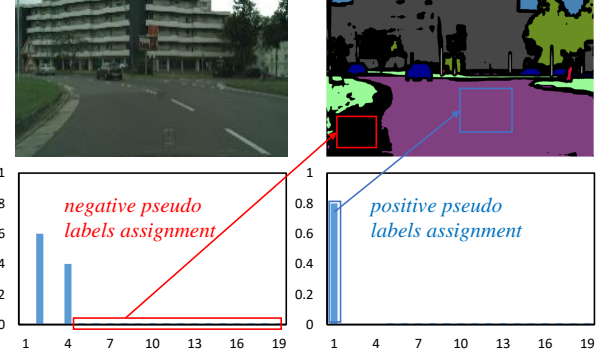


Figure 3. Bidirectional pseudo labels. Blue refers to positive pseudo labels and red refers to negative pseudo labels.

ignore pixels (black areas), but it is easy to determine which categories it does not belong to. Inspired by this, we propose a bidirectional self-training method that includes positive pseudo labeling and negative pseudo labeling.

Positive pseudo labeling. We first introduce the class-balanced positive pseudo labeling method, which aims to select reliable pseudo labels with high confidence scores for training. Considering the domain-transfer difficulty among different categories, generating pseudo labels according to high confidence will cause hard-to-transfer categories to be ignored. Because easy-to-transfer classes (*e.g.*, roads, buildings, walls, sky) usually have higher prediction confidence scores, while hard-to-transfer classes (*e.g.*, lights, signals, trains, bicycles) perform poorly. Consequently, we assign pseudo-labels based on the guidance of the category-level threshold inspired by [57] as below,

$$\hat{y}_{x_t}^{(h,w,c)} = \begin{cases} 1 & \text{if } c = (\operatorname{argmax}_c p_{x_t}^{(h,w,c)}) \cap (p_{x_t}^{(h,w,c)} > \lambda_c) \\ 0 & \text{otherwise,} \end{cases} \quad (4)$$

where λ_c is a category-level threshold that is determined by the top K predictions within the class c .

Then, we optimize the target model by minimize the categorical cross-entropy with every pseudo label \hat{y}_t :

$$\mathcal{L}_{ppl} = -\frac{1}{n_t} \sum_{i=1}^{n_t} \sum_{j=1}^{H \times W} \sum_{c=1}^C \hat{y}_t^{(i,j,c)} \log p_t^{(i,j,c)}, \quad (5)$$

where n_t is the number of target images, $p_t^{(i,j,c)}$ denotes the predicted category probability, and $\hat{y}_t^{(i,j,c)}$ is the corresponding pseudo label obtained from Eq. (4).

Negative pseudo labeling. For the negative pseudo-label assignment, our goal is to explore the implicit knowledge in uncertainty-aware regions that have been ignored in previous works. Although these predictions have higher uncertainty due to the uniform or low prediction scores, they can definitely point out the absent categories. For example, for a pixel whose output is [0.48, 0.47, 0.02, 0.03], it is impossible

to determine which category it belongs to, but we can confidently point out that it does not belong to classes with scores of 0.02 and 0.03. Therefore, we use all absent classes as supervision information for target feature learning. Formally, we assign the negative pseudo labels as follows:

$$\delta(p_{x_t}^{(h,w,c)}) = \begin{cases} 1 & \text{if } p_{x_t}^{(h,w,c)} < \lambda_{neg}, \\ 0 & \text{otherwise,} \end{cases} \quad (6)$$

where λ_{neg} is the negative threshold and we use $\lambda_{neg} = 0.05$ for all experiments. It is worth noticing that the negative pseudo labels are binary multi-labels, which certainly indicates the absence of relative classes. Then the negative pseudo labeling objective is formulated as follows:

$$\mathcal{L}_{npl} = -\frac{1}{n_t} \sum_{i=1}^{n_t} \sum_{j=1}^{H \times W} \sum_{c=1}^C \delta(p_t^{(i,j,c)}) \log(1 - p_t^{(i,j,c)}). \quad (7)$$

Finally, the bidirectional self-training objective includes the positive and negative pseudo labeling:

$$\mathcal{L}_{bst} = \mathcal{L}_{ppl} + \mathcal{L}_{npl}. \quad (8)$$

3.3. Information Propagation

Even we propose a much better solution for global adaptation without source data, intra-domain discrepancy still exists, as previous works [25, 31] indicate. Inspired by the intra-domain alignment method [31], we first divide the target data into easy and hard splits and then close the intra-domain gap to boost the adaptation performance. Contrary to the traditional adversarial mechanism, we borrow a semi-supervised learning scheme by considering the easy split as labeled data and the hard split unlabeled. As such, the target domain is separated using the entropy ranking strategy as below,

$$r(x_t) = \frac{1}{HW} \sum_{h=1}^H \sum_{w=1}^W h(x_t)^{(h,w)}, \quad (9)$$

which is the mean entropy for a target image x_t with the corresponding entropy map $h(x_t)$. Easy and hard splits are conducted from the ranking of $r(x_t)$ following $ratio = \frac{\|x_{te}\|}{(\|x_{te}\| + \|x_{th}\|)}$, where x_{te} and x_{th} denote the easy and hard samples, respectively.

After that, we conduct a proxy semi-supervised learning task based on the assumption that it is necessary to mitigate intra-domain discrepancy and pseudo labels of the easy part are reliable. We borrow semi-supervised learning techniques to bridge the intra-domain gap. We incorporate dominant semi-supervised learning approaches, including consistency-based methods [30, 47] and contrastive learning methods [24], and propose the following propagation objective:

$$\begin{aligned} \mathcal{L}_{ssl} = & \mathcal{L}_{ce}(\mathcal{M}_t(x_{te}), \hat{y}_{te}) + \\ & \mathcal{L}_{cyc}(\mathcal{M}_t(\text{Aug}(x_{th})), \mathcal{M}'_t(x_{th})), \end{aligned} \quad (10)$$

where \hat{y}_{te} denotes the pseudo labels of x_{te} obtained from the trained model in Eq. (8). \mathcal{L}_{ce} is the cross-entropy loss and \mathcal{L}_{cyc} is the consistency loss [47]. $\text{Aug}(x)$ denotes data augmentation operation for image x . \mathcal{M}'_t offers the values of target model \mathcal{M}_t without gradient optimization.

Unlike the most closely related work [31] that reduces intra-domain gap by conducting intra-domain adversarial learning, our framework directly learns consistency representations for the target data in a semi-supervised learning manner. Notice that the adopted technique can be considered as a standard post-process for adaptation, which is more simple and stable than the adversarial learning method.

4. Experiments

4.1. Datasets

We demonstrate the efficacy of the proposed method on the standard adaptation tasks of GTA5 [33]→Cityscapes [9], SYNTHIA [34]→Cityscapes and Cityscapes→NTHU Cross-City [6]. The synthetic dataset GTA5 contains 24,966 annotated images with a resolution of 1914×1052 , token from the famous game Grand Theft Auto. The ground truth is generated by the game render itself. SYNTHIA is another synthetic dataset, which contains 9,400 fully annotated images with the resolution of 1280×760 . Cityscapes consists 2,975 annotated training images, and 500 validation images with the resolution of 2048×1024 . NTHU Cross-City dataset has been recorded in four cities: Rome, Rio, Tokyo, and Taipei. Each city set has 3,200 unlabeled training images and 100 testing images with the resolution of 2048×1024 . We employ the mean Intersection over Union (mIoU) as the evaluation metric which is widely adopted in semantic segmentation tasks.

4.2. Implementation Details

We use the DeepLab [3] architecture with ResNet-101 [11] pre-trained on ImageNet [10] as the backbone, which is the same as previous works [27, 40, 43]. We first pre-train the segmentation network on the source domain for 80k iterations to obtain a high-quality source model. Then it is considered as the initialization model. During training, we follow previous works [27, 40, 43] using Stochastic Gradient Descent (SGD) optimizer with the learning rate 2.5×10^{-4} , momentum 0.9, and weight decay 5×10^{-4} . We schedule the learning rate using “poly” policy: the learning rate is multiplied by $(1 - \frac{iter}{max_iter})^{0.9}$. In the entropy minimization stage, we fix the classifier as above mentioned. In the other stages, the classifier is optimized with the learning rate 2.5×10^{-3} . Concerning the parameters, we utilize $\alpha = 0.002$, $\gamma = 3$, and $\lambda_{neg} = 0.05$ for all experiments. For self-training process, we assign the category-level top $K = 65\%$ target predictions as pseudo-labels. We update pseudo labels epoch by epoch, and the maximum number

Table 1. Results of GTA5 → Cityscapes (CS). “SF” denotes the source data-free setting. **Blue** is the best result for source data-free methods.

Method	SF	road	side.	build.	wall	fence	pole	light	sign	vege.	terr.	sky	person	rider	car	truck	bus	train	motor.	bike	mIoU
AdaptSeg [40]	✗	86.5	36.0	79.9	23.4	23.3	23.9	35.2	14.8	83.4	33.3	75.6	58.5	27.6	73.7	32.5	35.4	3.9	30.1	28.1	42.4
ADVENT [43]	✗	89.4	33.1	81.0	26.6	26.8	27.2	33.5	24.7	83.9	36.7	78.8	58.7	30.5	84.8	38.5	44.5	1.7	31.6	32.4	45.5
CBST [57]	✗	91.8	53.5	80.5	32.7	21.0	34.0	28.9	20.4	83.9	34.2	80.9	53.1	24.0	82.7	30.3	35.9	16.0	25.9	42.8	45.9
MaxSquare [4]	✗	89.4	43.0	82.1	30.5	21.3	30.3	34.7	24.0	85.3	39.4	78.2	63.0	22.9	84.6	36.4	43.0	5.5	34.7	33.5	46.4
CAG_UDA [53]	✗	90.4	51.6	83.8	34.2	27.8	38.4	25.3	48.4	85.4	38.2	78.1	58.6	34.6	84.7	21.9	42.7	41.1	29.3	37.2	50.2
SFDA [25]	✓	84.2	39.2	82.7	27.5	22.1	25.9	31.1	21.9	82.4	30.5	85.3	58.7	22.1	80.0	33.1	31.5	3.6	27.8	30.6	43.2
URMA [35]	✓	92.3	55.2	81.6	30.8	18.8	37.1	17.7	12.1	84.2	35.9	83.8	57.7	24.1	81.7	27.5	44.3	6.9	24.1	40.4	45.1
S4T [32]	✓	89.7	39.2	84.4	25.7	29.0	39.5	45.1	36.8	86.8	41.8	79.3	61.2	26.7	85.0	19.3	28.2	5.3	11.8	9.3	44.8
SFUDA [50]	✓	95.2	40.6	85.2	30.6	26.1	35.8	34.7	32.8	85.3	41.7	79.5	61.0	28.2	86.5	41.2	45.3	15.6	33.1	40.0	49.4
HCL [14]	✓	92.0	55.0	80.4	33.5	24.6	37.1	35.1	28.8	83.0	37.6	82.3	59.4	27.6	83.6	32.3	36.6	14.1	28.7	43.0	48.1
ATP (w/o TP)	✓	90.1	33.7	83.7	31.5	20.6	31.7	34.5	25.4	84.8	38.2	82.0	59.9	26.9	84.5	25.9	38.9	6.9	23.8	32.1	45.0
ATP (w/o P)	✓	90.4	43.9	85.1	40.4	23.8	34.2	41.8	34.3	84.2	35.9	85.5	62.3	21.9	83.8	36.9	51.8	0.0	36.8	53.0	49.8
ATP	✓	93.2	55.8	86.5	45.2	27.3	36.6	42.8	37.9	86.0	43.1	87.9	63.5	15.3	85.5	41.2	55.7	0.0	38.1	57.4	52.6

Table 2. Results of SYNTHIA → Cityscapes. “SF” denotes the source data-free setting. **Blue** is the best result for source data-free methods.

Method	SF	road	side.	build.	wall*	fence*	pole*	light	sign	vege.	sky	person	rider	car	bus	motor.	bike	mIoU	mIoU*
AdaptSeg [40]	✗	79.2	37.2	78.8	-	-	-	9.9	10.5	78.2	80.5	53.5	19.6	67.0	29.5	21.6	31.3	-	45.9
ADVENT [43]	✗	85.6	42.2	79.7	8.7	0.4	25.9	5.4	8.1	80.4	84.1	57.9	23.8	73.3	36.4	14.2	33.0	41.2	48.0
CBST [57]	✗	68.0	29.9	76.3	10.8	1.4	33.9	22.8	29.5	77.6	78.3	60.6	28.3	81.6	23.5	18.8	39.8	42.6	48.9
MaxSquare [4]	✗	82.9	40.7	80.3	10.2	0.8	25.8	12.8	18.2	82.5	82.2	53.1	18.0	79.0	31.4	10.4	35.6	41.4	48.2
CAG_UDA [53]	✗	84.8	41.7	85.5	-	-	-	13.7	23.0	86.5	78.1	66.3	28.1	81.8	21.8	22.9	49.0	-	52.6
SFDA [25]	✓	81.9	44.9	81.7	4.0	0.5	26.2	3.3	10.7	86.3	89.4	37.9	13.4	80.6	25.6	9.6	31.3	39.2	45.9
URMA [35]	✓	59.3	24.6	77.0	14.0	1.8	31.5	18.3	32.0	83.1	80.4	46.3	17.8	76.7	17.0	18.5	34.6	39.6	45.0
S4T [32]	✓	84.9	43.2	79.5	7.2	0.3	26.3	7.8	11.7	80.7	82.4	52.4	18.7	77.4	9.6	9.5	37.9	39.3	45.8
SFUDA [50]	✓	90.9	45.5	80.8	3.6	0.5	28.6	8.5	26.1	83.4	83.6	55.2	25.0	79.5	32.8	20.2	43.9	44.2	51.9
HCL [14]	✓	80.9	34.9	76.7	6.6	0.2	36.1	20.1	28.2	79.1	83.1	55.6	25.6	78.8	32.7	24.1	32.7	43.5	50.2
ATP (w/o TP)	✓	89.7	44.6	80.1	3.3	0.3	28.4	8.1	7.7	81.1	85.2	55.2	19.1	83.4	34.3	16.7	32.4	41.8	49.0
ATP (w/o P)	✓	89.8	45.1	82.9	0.1	0.0	33.8	14.6	17.3	84.5	87.0	59.3	25.6	85.8	49.4	26.2	56.1	46.9	55.9
ATP	✓	90.1	46.3	82.5	0.0	0.1	31.7	10.7	17.9	85.1	87.7	64.6	34.6	86.4	54.8	33.7	58.3	49.0	57.9

of epochs is empirically set as 10. For the semi-supervised training process, we assign the target images with average entropy ranked top 50% as the easy group, and the other images are defined as the hard group. Generally, we randomly run our methods three times with different random seeds via PyTorch and report the average accuracy.

4.3. Results

We show the performance of the proposed **ATP** on GTA5 → Cityscapes (CS) in Table 1, SYNTHIA → Cityscapes in Table 2, and Cityscapes → Cross-City (CC) in Table 3. **ATP (w/o TP)**, **ATP (w/o P)**, and **ATP** denote the results of different training stages, namely implicit feature alignment, bidirectional self-training, and information propagation, respectively. In addition, we compare our method with previ-

ous state-of-the-art works, including source data-dependent methods [4, 40, 43, 49, 53, 57] and source data-free methods [14, 25, 32, 35, 50]. The utility of source data can directly align distributions of source and target domains by adversarial learning [40, 43]. Thus they obtain higher performance reasonably. Notice that our method without source data performs comparable to or even better than the methods with source data. Furthermore, concerning source data-free methods, our method outperforms previous works [14, 25, 35] with a large margin. We visualize the masks predicted by our method in Figure 4.

Specifically, for the tasks of GTA5 → Cityscapes and SYNTHIA → Cityscapes, shown in Table 1 and 2, our method arrives at the mIoU score 52.6% and 57.9%, respectively, which offers a large margin performance gain compared with

Table 3. Results of CS → Cross-City with minor domain shift.

Method	SF	Rome	Rio	Tokyo	Taipei
ADVENT [43]	✗	47.3	46.8	45.5	45.1
AdaptSegNet [40]	✗	48.0	47.8	46.2	45.1
Cros-City [6]	✗	42.9	42.5	42.8	39.6
MaxSquare [4]	✗	48.5	48.7	47.1	47.2
SFDA [25]	✓	48.3	49.0	46.4	47.2
URMA [35]	✓	53.8	53.5	49.8	50.1
ATP (w/o TP)	✓	48.2	48.7	45.3	43.6
ATP (w/o P)	✓	53.8	55.3	48.6	47.8
ATP	✓	55.9	57.8	50.5	51.1

Table 4. Results of *black-box* source model on GTA5 → Cityscapes. “SF” denotes the source data-free setting.

Method	SF	BG	MC	RIV	RIG	DS	mIoU
AdatSegNet [40]	✗	53.2	22.4	24.6	61.3	50.0	42.2
ADVENT [43]	✗	55.6	24.1	28.5	61.3	56.6	45.5
CBST [57]	✗	55.5	27.2	27.8	72.7	50.5	45.9
MaxSquare [4]	✗	56.2	24.2	29.7	66.2	56.8	46.4
PLCA [15]	✗	57.3	28.3	31.1	57.2	60.2	47.7
SFDA [25]	✓	55.1	21.0	26.3	61.7	50.8	43.2
URMA [35]	✓	55.8	23.8	22.3	73.7	52.8	45.1
ATP (w/o P)	✓	51.1	28.0	27.7	49.2	40.9	40.4
ATP	✓	54.9	32.4	28.3	53.8	48.3	44.4
ATP (aug)	✓	55.6	37.2	30.9	54.7	50.7	45.3

the non-adaptation baseline. Moreover, the proposed method surpasses three existing source data-free methods SFDA [25], URMA [35] and HCL [14] by 9.4%, 7.5% and 4.5% mIoU scores on GTA5→Cityscapes, respectively. Compared with the adaptation methods using source data, our method even outperforms or achieves competitive results. These results verify the effectiveness of our method.

Table 3 shows the results on Cityscapes→Cross-City task. For clear description, we only report the mIoU scores in four different cities. The results demonstrate the effectiveness of our method for minor domain shift adaptation, achieving the best results in Rome, Rio, Tokyo, and Taipei.

4.4. Extension in Black-box Source Model

We also conduct experiments for the black-box source model [23], where only the source model’s predictions are available. Due to no access to a trained source model, the implicit feature alignment is impractical. Consequently, we apply our bidirectional self-training strategy and information propagation to tackle the black-box source model scenario. This situation is more challenging and interesting in practice, because it does not require any source model details but the network outputs. We report GTA5→Cityscapes results in Table 4. “ATP (w/o P)” and “ATP” represent our black-box

Table 5. Ablation study of each component on GTA5→CS task.

Model	\mathcal{L}_{cel}	\mathcal{L}_{div}	\mathcal{L}_{kld}	\mathcal{L}_{div}^*	\mathcal{L}_{ppl}	\mathcal{L}_{npl}	\mathcal{L}_{ssl}	mIoU
Baseline								39.3
(a)	✓							43.6
(b)	✓	✓						44.5
(c)	✓	✓	✓					45.0
(d)	✓			✓				43.9
(e)	✓	✓	✓		✓			47.7
(f)	✓	✓	✓		✓	✓		49.8
(g)	✓	✓	✓		✓	✓	✓	52.6

Table 6. Results on different SSL approaches on GTA5 → CS.

ratio	Baseline	CutMix [51]	ClassMix [30]	ReCo [24]
0.5	49.8	50.4	52.6	51.9
0.3	49.8	50.6	52.1	51.4

source model on the bidirectional self-training stage and information propagation stage, respectively. “ATP (aug)” denotes our results using data augmentation techniques. Due to space limitations, we report mean IoUs for *class-groups*¹ in this subsection. From the results, we can observe that our method is suitable for the black-box source model situation with a performance of 45.3%, comparable with source data-dependent and source data-free adaptation methods.

4.5. Ablation Study

In Table 5, we use the normal entropy minimization as our baseline model. The compared results reveal the improvement of proposed components on GTA5→Cityscapes task by progressively adding each module into the system.

Influence of implicit feature alignment. From the models (a) and (b) in Table 5, we can observe that our curriculum-style entropy loss (\mathcal{L}_{cel}) and weighted diversity loss (\mathcal{L}_{div}) can significantly improve adaptation performance. Specifically, model (a) with \mathcal{L}_{cel} achieves a 43.6% mIoU result, which surpasses the baseline model by 4.3 points. Furthermore, model (b) with \mathcal{L}_{div} boosts the performance improvement with 0.9 mIoU, revealing that diversity enforcing is important for our setting. We also utilize model regularized KL divergence [56] constraint (\mathcal{L}_{kld}) to provide 0.5 mIoU gains, as model (c) shows. \mathcal{L}_{div}^* denotes diversity loss provided by [22] with the mean output embedding. Compared model (b) with (d), we see that both diversity-promoting terms are beneficial for our task, and the proposed weighted one (\mathcal{L}_{div}) works better than a non-weighted one (\mathcal{L}_{div}^*).

Influence of bidirectional self-training. We ablate the

¹Background (**BG**)-building, wall, fence, vegetation, terrain, sky; Minority Class (**MC**)-rider, train, motorcycle, bicycle; Road Infrastructure Vertical (**RIV**)-pole, traffic light, traffic sign; Road Infrastructure Ground (**RIG**)-road, sidewalk; and Dynamic Stuff (**DS**)-person, car, truck, bus.

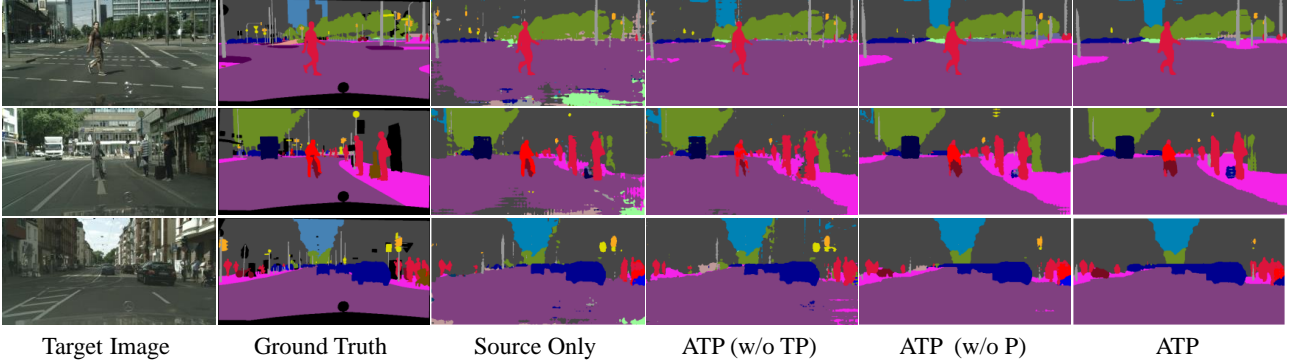


Figure 4. Visualization for predicted segmentation masks on the GTA5→Cityscapes task.

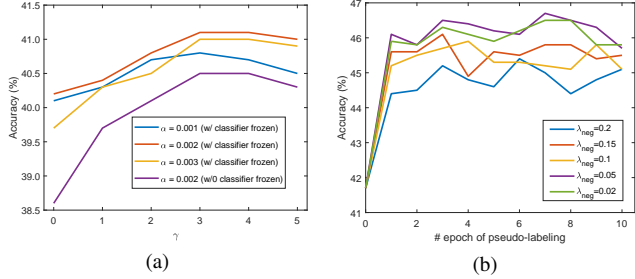


Figure 5. (a) Analysis for the hyper-parameters α and γ of the proposed adaptive entropy loss. (b) Robustness to the negative threshold λ_{neg} for the negative pseudo assignment method.

positive pseudo labeling \mathcal{L}_{ppl} and negative pseudo labeling \mathcal{L}_{npl} , respectively. The results show that model (e) trained from positive pseudo labeling provides 2.7 point gains compared to model (c). It is reasonable that the positive pseudo labels enhance feature representations for target data. On the other hand, the negative pseudo labeling (model (f)) fancily offers 2.1 point improvement based on the model (e). This result demonstrates that the uncertainty information is helpful to learn decision boundaries, and it is complementary to traditional positive labeling methods.

Influence of information propagation. To testify the effectiveness of the information propagation strategy, we follow several semi-supervised learning methods in our approach, including consistency learning technique (Cut-Mix [51], ClassMix [30]) and contrastive learning technique (ReCo [24]). We report the best result obtained from ClassMix model (g) in Table 5, which provides a significant improvement with 2.8 mIoU compared to model (f). Detailed results of the information propagation stage are shown in Table 6. The parameter *ratio* denotes the proportion of easy split on the whole target dataset.

4.6. Parameter Sensitivity Analysis

Our framework contains two new hyper-parameters α and γ in Eq. (2). To analyze the influence, we conduct experiments on the GTA5→Cityscapes task. We select the value of

α from the range of [0.001, 0.002, 0.003], γ from the range of [0, 1, 2, 3, 4, 5], respectively. The results are shown in Figure 5a. Although all experiments set $\alpha = 0.002$ and $\gamma = 3$ since it peaks, we observe that the proposed curriculum-style entropy loss is relatively robust to these parameters. Furthermore, we also optimize the model without freezing the source classifier. The performance drops significantly compared to those with frozen classifier, which indicates that the hypothesis transfer with frozen classifier is essential.

Figure 5b shows the test accuracy when varying the assignment threshold λ_{neg} related to negative pseudo labels in Eq. (6). It shows that the proposed negative pseudo labeling method is relatively robust to this hyper-parameter. Moreover, the proposed method quickly converges after several training epochs. We also observe that $\lambda_{neg} < 0.1$ obtains a satisfactory performance compared to those when $\lambda_{neg} > 0.1$. This may be because that more noise labels are introduced when the threshold increases because our negative pseudo labeling method focuses on the predictions with lower confidence scores.

Limitation. The main limitation is that it fails to handle some classes with a large domain gap or occupy a minor pixel proportion, like fence, pole, signal and train, as Table 1 and Table 2 show. It is a common limitation for DASS that may be caused by the class-imbalance problem.

5. Conclusion

This paper presents a novel source data-free framework for domain adaptive semantic segmentation called **ATP**. In the absence of source data, **ATP** focuses on transferring knowledge from the source model via implicit feature alignment, teaching from positive and negative pseudo labels, and propagating target-specific information to reduce the intra-domain discrepancy. Extensive experiments and ablation studies are conducted to validate the effectiveness of the proposed **ATP**. On the standard adaptation tasks, **ATP** achieves new state-of-the-art results and performs comparably to source data-dependent adaptation methods.

References

[1] David Berthelot, Nicholas Carlini, Ekin D Cubuk, Alex Kurakin, Kihyuk Sohn, Han Zhang, and Colin Raffel. Remixmatch: Semi-supervised learning with distribution alignment and augmentation anchoring. In *Proc. ICLR*, 2019. 3

[2] Wei-Lun Chang, Hui-Po Wang, Wen-Hsiao Peng, and Wei-Chen Chiu. All about structure: Adapting structural information across domains for boosting semantic segmentation. In *Proc. CVPR*, pages 1900–1909, 2019. 2

[3] Liang-Chieh Chen, George Papandreou, Iasonas Kokkinos, Kevin Murphy, and Alan L Yuille. Deeplab: Semantic image segmentation with deep convolutional nets, atrous convolution, and fully connected crfs. *IEEE Transactions on Pattern Analysis and Machine Intelligence*, 40(4):834–848, 2017. 5

[4] Minghao Chen, Hongyang Xue, and Deng Cai. Domain adaptation for semantic segmentation with maximum squares loss. In *Proc. ICCV*, pages 2090–2099, 2019. 1, 2, 6, 7

[5] Yun-Chun Chen, Yen-Yu Lin, Ming-Hsuan Yang, and Jia-Bin Huang. Crdoco: Pixel-level domain transfer with cross-domain consistency. In *Proc. CVPR*, pages 1791–1800, 2019. 2

[6] Yi-Hsin Chen, Wei-Yu Chen, Yu-Ting Chen, Bo-Cheng Tsai, Yu-Chiang Frank Wang, and Min Sun. No more discrimination: Cross city adaptation of road scene segmenters. In *Proc. ICCV*, pages 1992–2001, 2017. 5, 7

[7] Boris Chidlovskii, Stéphane Clinchant, and Gabriela Csurka. Domain adaptation in the absence of source domain data. In *Proc. KDD*, pages 451–460, 2016. 2

[8] Jaehoon Choi, Taekyung Kim, and Changick Kim. Self-ensembling with gan-based data augmentation for domain adaptation in semantic segmentation. In *Proc. ICCV*, pages 6830–6840, 2019. 2

[9] Marius Cordts, Mohamed Omran, Sebastian Ramos, Timo Rehfeld, Markus Enzweiler, Rodrigo Benenson, Uwe Franke, Stefan Roth, and Bernt Schiele. The cityscapes dataset for semantic urban scene understanding. In *Proc. CVPR*, pages 3213–3223, 2016. 2, 5

[10] Jia Deng, Wei Dong, Richard Socher, Li-Jia Li, Kai Li, and Li Fei-Fei. Imagenet: A large-scale hierarchical image database. In *Proc. CVPR*, pages 248–255, 2009. 5

[11] Kaiming He, Xiangyu Zhang, Shaoqing Ren, and Jian Sun. Deep residual learning for image recognition. In *Proc. CVPR*, pages 770–778, 2016. 5

[12] Judy Hoffman, Eric Tzeng, Taesung Park, Jun-Yan Zhu, Phillip Isola, Kate Saenko, Alexei Efros, and Trevor Darrell. CyCADA: Cycle-consistent adversarial domain adaptation. In *Proc. ICML*, pages 1989–1998, 2018. 1, 2

[13] Weixiang Hong, Zhenzhen Wang, Ming Yang, and Junsong Yuan. Conditional generative adversarial network for structured domain adaptation. In *Proc. CVPR*, pages 1335–1344, 2018. 1, 2

[14] Jiaxing Huang, Dayan Guan, Aoran Xiao, and Shijian Lu. Model adaptation: Historical contrastive learning for unsupervised domain adaptation without source data. *arXiv preprint arXiv:2110.03374*, 2021. 2, 6, 7

[15] Guoliang Kang, Yunchao Wei, Yi Yang, Yueling Zhuang, and Alexander Hauptmann. Pixel-level cycle association: A new perspective for domain adaptive semantic segmentation. In *Proc. NeurIPS*, pages 3569–3580, 2020. 2, 7

[16] Myeongjin Kim and Hyeran Byun. Learning texture invariant representation for domain adaptation of semantic segmentation. In *Proc. CVPR*, pages 12975–12984, 2020. 2

[17] Jogendra Nath Kundu, Akshay Kulkarni, Amit Singh, Varun Jampani, and R Venkatesh Babu. Generalize then adapt: Source-free domain adaptive semantic segmentation. In *Proc. ICCV*, pages 7046–7056, 2021. 2

[18] Jogendra Nath Kundu, Naveen Venkat, R Venkatesh Babu, et al. Universal source-free domain adaptation. In *Proc. CVPR*, pages 4544–4553, 2020. 2

[19] Rui Li, Qianfen Jiao, Wenming Cao, Hau-San Wong, and Si Wu. Model adaptation: Unsupervised domain adaptation without source data. In *Proc. CVPR*, pages 9641–9650, 2020. 2

[20] Qing Lian, Fengmao Lv, Lixin Duan, and Boqing Gong. Constructing self-motivated pyramid curriculums for cross-domain semantic segmentation: A non-adversarial approach. In *Proc. ICCV*, pages 6758–6767, 2019. 2

[21] Jian Liang, Ran He, Zhenan Sun, and Tieniu Tan. Distant supervised centroid shift: A simple and efficient approach to visual domain adaptation. In *Proc. CVPR*, pages 2975–2984, 2019. 1

[22] Jian Liang, Dapeng Hu, and Jiashi Feng. Do we really need to access the source data? source hypothesis transfer for unsupervised domain adaptation. In *Proc. ICML*, pages 6028–6039, 2020. 2, 4, 7

[23] Jian Liang, Dapeng Hu, Ran He, and Jiashi Feng. Distill and fine-tune: Effective adaptation from a black-box source model. *arXiv:2104.01539*, 2021. 7

[24] Shikun Liu, Shuaifeng Zhi, Edward Johns, and Andrew J Davison. Bootstrapping semantic segmentation with regional contrast. *arXiv preprint arXiv:2104.04465*, 2021. 5, 7, 8

[25] Yuang Liu, Wei Zhang, and Jun Wang. Source-free domain adaptation for semantic segmentation. In *Proc. CVPR*, pages 1215–1224, 2021. 2, 5, 6, 7

[26] Jonathan Long, Evan Shelhamer, and Trevor Darrell. Fully convolutional networks for semantic segmentation. In *Proc. CVPR*, pages 3431–3440, 2015. 1

[27] Yawei Luo, Liang Zheng, Tao Guan, Junqing Yu, and Yi Yang. Taking a closer look at domain shift: Category-level adversaries for semantics consistent domain adaptation. In *Proc. CVPR*, pages 2507–2516, 2019. 1, 2, 5

[28] Ke Mei, Chuang Zhu, Jiaqi Zou, and Shanghang Zhang. Instance adaptive self-training for unsupervised domain adaptation. In *Proc. ECCV*, pages 415–430, 2020. 2

[29] Takeru Miyato, Shin-ichi Maeda, Masanori Koyama, and Shin Ishii. Virtual adversarial training: a regularization method for supervised and semi-supervised learning. *IEEE Transactions on Pattern Analysis and Machine Intelligence*, 41(8):1979–1993, 2018. 3

[30] Viktor Olsson, Wilhelm Tranheden, Juliano Pinto, and Lennart Svensson. Classmix: Segmentation-based data augmentation for semi-supervised learning. In *Proc. WACV*, pages 1369–1378, 2021. 5, 7, 8

[31] Fei Pan, Inkyu Shin, Francois Rameau, Seokju Lee, and In So Kweon. Unsupervised intra-domain adaptation for semantic segmentation through self-supervision. In *Proc. ICCV*, pages 3764–3773, 2020. [3](#), [5](#)

[32] Viraj Prabhu, Shivam Khare, Deeksha Kartik, and Judy Hoffman. S4t: Source-free domain adaptation for semantic segmentation via self-supervised selective self-training. *arXiv preprint arXiv:2107.10140*, 2021. [6](#)

[33] Stephan R Richter, Vibhav Vineet, Stefan Roth, and Vladlen Koltun. Playing for data: Ground truth from computer games. In *Proc. ECCV*, pages 102–118, 2016. [2](#), [5](#)

[34] German Ros, Laura Sellart, Joanna Materzynska, David Vazquez, and Antonio M Lopez. The synthia dataset: A large collection of synthetic images for semantic segmentation of urban scenes. In *Proc. CVPR*, pages 3234–3243, 2016. [2](#), [5](#)

[35] Prabhu Teja S and Francois Fleuret. Uncertainty reduction for model adaptation in semantic segmentation. In *Proc. CVPR*, pages 9613–9623, 2021. [2](#), [6](#), [7](#)

[36] Kuniaki Saito, Donghyun Kim, Piotr Teterwak, Stan Sclaroff, Trevor Darrell, and Kate Saenko. Tune it the right way: Unsupervised validation of domain adaptation via soft neighborhood density. In *Proc. ICCV*, pages 9184–9193, 2021. [2](#)

[37] Swami Sankaranarayanan, Yogesh Balaji, Arpit Jain, Ser Nam Lim, and Rama Chellappa. Learning from synthetic data: Addressing domain shift for semantic segmentation. In *Proc. CVPR*, pages 3752–3761, 2018. [2](#)

[38] M Naseer Subhani and Mohsen Ali. Learning from scale-invariant examples for domain adaptation in semantic segmentation. In *Proc. ECCV*, pages 290–306, 2020. [2](#)

[39] Thanh-Dat Truong, Chi Nhan Duong, Ngan Le, Son Lam Phung, Chase Rainwater, and Khoa Luu. Bimal: Bijective maximum likelihood approach to domain adaptation in semantic scene segmentation. In *Proc. ICCV*, pages 8548–8557, 2021. [2](#)

[40] Yi-Hsuan Tsai, Wei-Chih Hung, Samuel Schulter, Kihyuk Sohn, Ming-Hsuan Yang, and Manmohan Chandraker. Learning to adapt structured output space for semantic segmentation. In *Proc. CVPR*, pages 7472–7481, 2018. [1](#), [2](#), [5](#), [6](#), [7](#)

[41] Yi-Hsuan Tsai, Kihyuk Sohn, Samuel Schulter, and Manmohan Chandraker. Domain adaptation for structured output via discriminative patch representations. In *Proc. ICCV*, pages 1456–1465, 2019. [2](#)

[42] Vikas Verma, Alex Lamb, Juho Kannala, Yoshua Bengio, and David Lopez-Paz. Interpolation consistency training for semi-supervised learning. In *Proc. IJCAI*, pages 3635–3641, 2019. [3](#)

[43] Tuan-Hung Vu, Himalaya Jain, Maxime Bucher, Matthieu Cord, and Patrick Pérez. Advent: Adversarial entropy minimization for domain adaptation in semantic segmentation. In *Proc. CVPR*, pages 2517–2526, 2019. [1](#), [2](#), [3](#), [5](#), [6](#), [7](#)

[44] Yuxi Wang, Junran Peng, and ZhaoXiang Zhang. Uncertainty-aware pseudo label refinery for domain adaptive semantic segmentation. In *Proc. ICCV*, pages 9092–9101, 2021. [1](#), [2](#), [4](#)

[45] Zuxuan Wu, Xin Wang, Joseph E Gonzalez, Tom Goldstein, and Larry S Davis. Ace: Adapting to changing environments for semantic segmentation. In *Proc. ICCV*, pages 2121–2130, 2019. [2](#)

[46] Haifeng Xia, Handong Zhao, and Zhengming Ding. Adaptive adversarial network for source-free domain adaptation. In *Proc. ICCV*, pages 9010–9019, 2021. [2](#)

[47] Qizhe Xie, Zihang Dai, Eduard Hovy, Thang Luong, and Quoc Le. Unsupervised data augmentation for consistency training. In *Proc. NeurIPS*, pages 6256–6268, 2020. [3](#), [5](#)

[48] Shiqi Yang, Yaxing Wang, Joost van de Weijer, Luis Herranz, and Shangling Jui. Generalized source-free domain adaptation. In *Proc. ICCV*, pages 8978–8987, 2021. [2](#)

[49] Yanchao Yang and Stefano Soatto. Fda: Fourier domain adaptation for semantic segmentation. In *Proc. CVPR*, pages 4085–4095, 2020. [1](#), [2](#), [6](#)

[50] Mucong Ye, Jing Zhang, Jinpeng Ouyang, and Ding Yuan. Source data-free unsupervised domain adaptation for semantic segmentation. In *Proc. ACM MM*, pages 2233–2242, 2021. [2](#)

[51] Sangdoo Yun, Dongyoon Han, Seong Joon Oh, Sanghyuk Chun, Junsuk Choe, and Youngjoon Yoo. Cutmix: Regularization strategy to train strong classifiers with localizable features. In *Proc. ICCV*, pages 6023–6032, 2019. [7](#), [8](#)

[52] Pan Zhang, Bo Zhang, Ting Zhang, Dong Chen, Yong Wang, and Fang Wen. Prototypical pseudo label denoising and target structure learning for domain adaptive semantic segmentation. In *Proc. CVPR*, pages 12414–12424, 2021. [2](#), [4](#)

[53] Qiming Zhang, Jing Zhang, Wei Liu, and Dacheng Tao. Category anchor-guided unsupervised domain adaptation for semantic segmentation. In *Proc. NeurIPS*, pages 433–443, 2019. [6](#)

[54] Yang Zhang, Philip David, and Boqing Gong. Curriculum domain adaptation for semantic segmentation of urban scenes. In *Proc. ICCV*, pages 2020–2030, 2017. [2](#), [3](#)

[55] Zhedong Zheng and Yi Yang. Rectifying pseudo label learning via uncertainty estimation for domain adaptive semantic segmentation. *International Journal of Computer Vision*, 129(4):1106–1120, 2021. [2](#)

[56] Yang Zou, Zhiding Yu, Xiaofeng Liu, BVK Kumar, and Jinsong Wang. Confidence regularized self-training. In *Proc. ICCV*, pages 5982–5991, 2019. [2](#), [7](#)

[57] Yang Zou, Zhiding Yu, BVK Vijaya Kumar, and Jinsong Wang. Unsupervised domain adaptation for semantic segmentation via class-balanced self-training. In *Proc. ECCV*, pages 289–305, 2018. [2](#), [3](#), [4](#), [6](#), [7](#)